

Internal Note No. 68-FM-298



NATIONAL AERONAUTICS AND SPACE ADMINISTRATION

N.I.

MSC INTERNAL NOTE NO. 68-FM-298

December 13, 1968

APOLLO 8 SPACECRAFT DISPERSION ANALYSIS

VOLUME I - DISPERSION SUMMARY

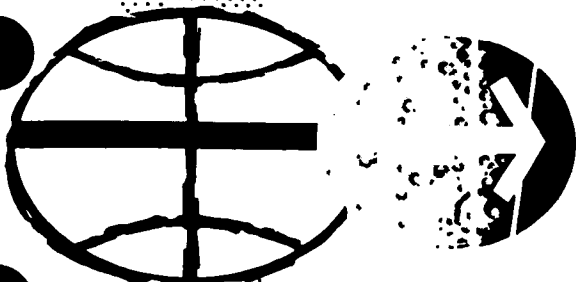


FEB 14 1969

Guidance and Performance Branch

MISSION PLANNING AND ANALYSIS DIVISION

MANNED SPACECRAFT CENTER
HOUSTON, TEXAS



(NASA-TM-X-69746) APOLLO 8 SPACECRAFT
DISPERSION ANALYSIS. VOLUME 1:
DISPERSION SUMMARY (NASA) 34 p

N74-70686

Unclassified
00/99 16331

MSC INTERNAL NOTE NO. 68-FM-298

PROJECT APOLLO

APOLLO 8 SPACECRAFT DISPERSION ANALYSIS
VOLUME I - DISPERSION SUMMARY

By R. Leroy McHenry
Guidance and Performance Branch

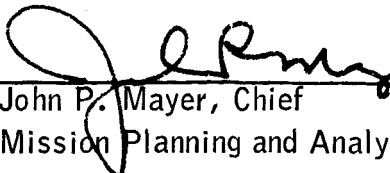
December 13, 1968

MISSION PLANNING AND ANALYSIS DIVISION
NATIONAL AERONAUTICS AND SPACE ADMINISTRATION
MANNED SPACECRAFT CENTER
HOUSTON, TEXAS

Approved:


Marlowe D. Cassetti, Chief
Guidance and Performance Branch

Approved:


John P. Mayer, Chief
Mission Planning and Analysis Division

FOREWORD

This study was prepared with a venting uncertainty of .0125 as a 1σ error. Subsequent to this analysis it was determined that this magnitude of venting uncertainty was about three times larger than the worst expected venting. Consequently, the information contained in this report for the translunar dispersion is approximately two to three times larger than expected. However, due to this and other analyses for this mission, it is recommended that, whenever possible, the venting be inhibited.

CONTENTS

| Section | Page |
|------------------------------------|------|
| SUMMARY | 1 |
| INTRODUCTION | 1 |
| SYMBOLS | 3 |
| COORDINATE SYSTEMS | 3 |
| SUMMARY OF ERROR SOURCES | 4 |
| COVARIANCE MATRIX FORMAT | 5 |
| DISCUSSION OF RESULTS | 5 |
| TLI | 5 |
| MCC-1 | 5 |
| MCC-2 | 6 |
| MCC-3 | 6 |
| MCC-4 | 6 |
| LOI(1) | 7 |
| LOI(2) | 7 |
| TEI | 7 |
| Transearch Phase | 7 |
| CONCLUSIONS | 8 |
| REFERENCES | 29 |

TABLES

| Table | | Page |
|-------|--|------|
| I | COVARIANCE MATRIX OF ACTUAL STATE VECTOR DEVIATIONS AT TLI CUTOFF-PLUS-15-MINUTES | |
| | (a) Covariance matrix | 9 |
| | (b) State vector deviations | 9 |
| II | COVARIANCE MATRIX OF ACTUAL STATE VECTOR UNCERTAINTIES AT NOMINAL LOI(1) IGNITION | |
| | (a) Covariance matrix | 10 |
| | (b) State vector deviations | 10 |
| III | COVARIANCE MATRIX OF ACTUAL STATE VECTOR DEVIATIONS AT NOMINAL LOI(2) IGNITION | |
| | (a) Covariance matrix | 11 |
| | (b) State vector deviations | 11 |
| IV | COVARIANCE MATRIX OF ACTUAL STATE VECTOR DEVIATIONS AT NOMINAL TEI IGNITION | |
| | (a) Covariance matrix | 12 |
| | (b) State vector deviations | 12 |
| V | COVARIANCE MATRIX OF ACTUAL STATE VECTOR DEVIATIONS AT NOMINAL TEI CUTOFF-PLUS-10-SECONDS | |
| | (a) Covariance matrix | 13 |
| | (b) State vector deviations | 13 |
| VI | TRANSLUNAR INJECTION DISPERSIONS | 14 |
| VII | TRANSLUNAR MCC-1 DISPERSIONS | 15 |
| VIII | TRANSLUNAR MCC-2 DISPERSIONS | 16 |
| IX | TRANSLUNAR MCC-3 DISPERSIONS | 17 |
| X | TRANSLUNAR MCC-4 DISPERSIONS | 18 |
| XI | SUMMARY OF TRANSLUNAR PHASE DISPERSION RESULTS | 19 |
| XII | LOI(1) DISPERSIONS | 20 |

| Table | | Page |
|-------|--|------|
| XIII | LOI(2) DISPERSIONS | 21 |
| XIV | TEI DISPERSIONS | 22 |
| XV | TRANSEARTH MCC-1 DISPERSIONS | 23 |
| XVI | TRANSEARTH MCC-2 DISPERSIONS | 24 |
| XVII | TRANSEARTH MCC-3 DISPERSIONS | 25 |
| XVIII | TRANSEARTH MCC-4 DISPERSIONS | 26 |
| XIX | REENTRY DISPERSIONS | 27 |
| XX | SUMMARY OF TRANSEARTH PHASE DISPERSIONS RESULTS | 27 |

APOLLO 8 SPACECRAFT DISPERSION ANALYSIS

VOLUME I - DISPERSION SUMMARY

By R. Leroy McHenry

SUMMARY

A spacecraft dispersion analysis for the Apollo 8 mission is presented in this report. The first phase of the dispersion analysis consists of translunar midcourse corrections performed by either the SPS or RCS engines of the CSM. The second phase begins at the lunar orbit insertion maneuver [LOI(1)] and is followed by the circularization maneuver [LOI(2)] and the transearth injection maneuver (TEI). The third trajectory phase is the transearth portion which also consists of midcourse corrections, and the final phase is reentry, which begins with entry interface and terminates at landing.

A continuous spacecraft vent of 0.0125 lb of thrust was simulated in the dispersion analysis and applied along the velocity vector during the translunar coast period. The analysis indicates that a ± 72 -n. mi. ($\pm 3\sigma$) dispersion in the pericynthion altitude after the first midcourse correction can be attributed to the effect of this spacecraft venting on the increased navigation uncertainties. The 3σ dispersion in pericynthion altitude after the second and third midcourse maneuvers is reduced considerably. After the fourth midcourse, this uncertainty is ± 20 n. mi. ($\pm 3\sigma$). Venting of this magnitude and in the direction along the velocity vector is a worst case condition.

Another important consideration is the fact that for SPS burns of less than 6-seconds duration, the CMC short burn logic does not represent the performance of the particular SPS engine used for this mission. Therefore, V_g residuals that are a function of the burn time will occur for maneuvers of this type.

INTRODUCTION

This dispersion analysis was performed on the Apollo 8 mission as defined in reference 1. Two hundred random translunar trajectories

were simulated for the end to end dispersion analysis of the first phase of the Apollo 8 mission. Each simulation was initiated with random state vector errors which were obtained from the covariance matrix of actual TLI state vector deviations (table I). Translunar midcourse corrections were targeted for nominal position and time of nodal passage of the approach hyperbola and the lunar orbit plane. The simulations include not only the effects of MSFN navigation errors and midcourse execution errors, but also the effects of continuous spacecraft venting. The amount of thrust due to venting was randomized to be approximately 0.0125 lb and applied along the velocity vector for each simulation.

The dispersion analyses of the LOI(1) maneuver, LOI(2) maneuver, and the transearth injection maneuver were performed by simulating 200 powered-flight trajectories for each maneuver. Covariance matrices (tables II, III, and IV) were used in initializing the state vector errors. These errors in initial conditions are the MSFN navigation uncertainties. The Mathematical Physics Branch (Mission Planning and Analysis Division) supplied these covariance matrices.

The transearth end-to-end dispersion analysis was performed in a manner similar to the translunar dispersion analysis. The covariance matrix (table V) was obtained from the TEI dispersion analysis and used to obtain initial state vector errors for the transearth dispersion analysis.

Transearth midcourse corrections were targeted to the nominal entry flight-path angle. Only the effects of navigation errors and midcourse errors were simulated. Spacecraft venting was not modeled for the transearth simulations.

The launch pad REFSMMAT was used to align the PGNCS for the first three midcourse maneuvers of the translunar phase. For the fourth translunar midcourse correction (MCC-4), LOI(1), LOI(2), TEI, and the first three transearth midcourse correction maneuvers, the LOI(2) preferred REFSMMAT was used. For the fourth transearth midcourse correction and reentry phase, the entry REFSMMAT was used. All maneuvers were simulated under the control of the PGNCS.

The translunar and transearth midcourse corrections summarized in tables VII through X and XV through XVIII represent the dispersions for the largest targets (ref. 2) for each maneuver. These are presented as they are indicative of the largest dispersions for the IMU.

SYMBOLS

| | |
|-----------|---|
| CMC | command module computer |
| CSM | command and service modules |
| IMU | inertial measurement unit |
| LOI(1) | lunar orbit insertion |
| LOI(2) | lunar orbit circularization |
| MCC | midcourse correction |
| MSFN | Manned Space Flight Network |
| PGNCS | primary guidance and navigation control system |
| PGNCS/DAP | PGNCS digital autopilot |
| REFSMMAT | reference stable member matrix |
| RCS | reaction control system |
| SPS | service propulsion system |
| S-IVB | Saturn IVB launch vehicle |
| TEI | transearth injection |
| TLI | translunar injection |
| v_g | velocity to be gained whose components are $(v_g)_x$, $(v_g)_y$ and $(v_g)_z$ |

COORDINATE SYSTEMS

The coordinate systems used are as follows:

Local vertical/local horizontal coordinates:

$$\bar{x} = (\bar{r} \times \bar{v}) \times \bar{r}$$

$$\bar{y} = \bar{z} \times \bar{x}$$

$$\bar{z} = -\bar{r}$$

u-v-w coordinates

$$u = \bar{r}$$

$$\mathbf{v} = \mathbf{u} \times \mathbf{w}$$

$$\mathbf{w} = \mathbf{u} \times \mathbf{v}$$

where \bar{r} = position vector in inertial coordinates

\bar{v} = velocity vector in inertial coordinates

SUMMARY OF ERROR SOURCES

The following is a summary of the error sources used in the dispersion analysis. All values are 1σ .

IMU platform misalignments

Accelerometer errors (PGNCS):

| | |
|---|------------------------|
| Biases (X, Y, Z), ft/sec ² | 0.00656 |
| Misalignments (XY, XZ, YX, YZ, ZX, ZY), (deg/sec)/(ft/sec) | 0.00556 |
| Scale factor (X, Y, Z) | 0.000116 |
| Nonlinearity coefficient (X, Y, Z) | 3.125×10^{-7} |

Gyro errors (PGNCS):

| | |
|--|------------------------|
| Bias drift (X, Y, Z), deg/sec | 8.356×10^{-6} |
| Unbalance in gyro input axis (X, Y, Z), (deg/sec)/(ft/sec ²) | 1.039×10^{-6} |
| Unbalance in gyro spin reference axis (X, Y, Z), (deg/sec)/(ft/sec ²) | 6.488×10^{-7} |

Vehicle performance errors:

| | |
|---------------------------------------|--------|
| Initial misalignment (pitch and yaw), | |
| deg | 0.167 |
| SPS thrust, lb | 66.9 |
| SPS specific impulse, sec | 0.531 |
| SPS tailoff uncertainty, sec | 0.040 |
| SPS engine mistrim (pitch and yaw), | |
| deg | 0.333 |
| Centrifugal thrust of CSM, lb | 0.0125 |

COVARIANCE MATRIX FORMAT

The format for the symmetric covariance matrices (u-v-w coordinates) is as follows:

$$\begin{bmatrix} \sigma_u \sigma_u \\ \sigma_u \sigma_v & \sigma_v \sigma_v \\ \sigma_u \sigma_w & \sigma_v \sigma_w & \sigma_w \sigma_w \\ \sigma_u \sigma_u^* & \sigma_v \sigma_u^* & \sigma_w \sigma_u^* & \sigma_u^* \sigma_u^* \\ \sigma_u \sigma_v^* & \sigma_v \sigma_v^* & \sigma_w \sigma_v^* & \sigma_u^* \sigma_v^* & \sigma_v^* \sigma_v^* \\ \sigma_u \sigma_w^* & \sigma_v \sigma_w^* & \sigma_w \sigma_w^* & \sigma_u^* \sigma_w^* & \sigma_v^* \sigma_w^* & \sigma_w^* \sigma_w^* \end{bmatrix}$$

DISCUSSION OF RESULTS

TLI

The 3σ deviations at TLI cutoff are presented in table VI. A covariance matrix of state vector deviations caused by launch vehicle dispersions is presented in table I. Initial state vector errors for the translunar trajectory dispersion analysis were randomized from this covariance matrix.

MCC-1

The first translunar midcourse correction is presented in table VII and represents the first midcourse correction at TLI-plus-6-hours. The maneuver presented is representative of SPS burns of greater than 6-seconds duration. For maneuvers of this type guidance commands are issued and the tailoff impulse is adequately compensated for. In table VII the 0.44 fps (v_g)_x residual is due to the uncertainty in tailoff impulse, while the (v_g)_y and (v_g)_z residuals are cross-axis velocity errors.

The 3σ uncertainty in pericynthion altitude of 72 n. mi. is primarily due to continuous spacecraft venting along the velocity vector during translunar flight. If venting along the velocity vector is realistic, then with no other corrections lunar impact could occur.

MCC-2

Table VIII shows that large middle gimbal angles can occur during the translunar phase if the launch pad REFSMMAT is used for MCC-2 as a reference to align the PGNCS. The maneuver presented was performed by two RCS jets. The 3σ uncertainty in pericynthion altitude after the second translunar midcourse correction maneuver is 38.6 n. mi. The large pericynthion altitude deviation is primarily caused by the translunar venting.

MCC-3

The largest maneuver required for the third translunar midcourse correction at 22 hours before is a LOI(1) SPS minimum-impulse maneuver and is presented in table IX. Even though the target for the maneuver is 5.34 fps the mean incremental velocity achieved is 7.47 fps. The velocity residual, -2.13 fps, occurs because the CMC short burn logic does not represent the performance of the SPS engine used. Furthermore, a 0.14-second delay in SPS engine cutoff was included. The 3σ deviation in pericynthion altitude after the third translunar midcourse correction maneuver is $\pm 3^{\frac{1}{4}}$ n. mi. and is due to the spacecraft venting.

MCC-4

Table X presents data for the fourth translunar midcourse maneuver at 8 hours before LOI(1). The CMC-calculated burn time for this maneuver is 2.72 seconds, which lies in the range (1 to 6 seconds) for the SPS short burn logic. No guidance steering commands are issued for maneuvers of this type. The CMC compensates for the total impulse equivalent to an SPS engine which has a 20 500 lb-thrust and a propellant flow rate of 63.8 lb/sec. However, the SPS thrust and propellant flow rate in reference 3 is 20 908 lb and 66.543 lb/sec, respectively. Therefore, a total impulse residual which is not compensated for by the CMC short burn logic will cause a velocity residual for all SPS burns of this type. For this particular maneuver, a 5.47-fps overburn occurs. Larger residuals occur for other maneuvers whose burn time lies in the range of the SPS short logic. Reference 4 presents velocity residuals which are a function of the burn time for all SPS burns of this type for the Apollo 8 mission.

The 3σ deviation in pericynthion altitude following the fourth translunar midcourse correction maneuver is ± 20 n. mi. The effect of venting along the velocity vector on the MSFN navigation uncertainties during translunar coast is the primary cause of pericynthion uncertainties. A detailed analysis of the translunar phase dispersions is presented in reference 2 and is summarized in table XI.

LOI(1)

The covariance matrix given in table II considers the uncertainty in the state vector at LOI(1) ignition. This uncertainty is due only to MSFN navigation errors and venting during the translunar coast. Actual state vector dispersions due to midcourse correction errors are not included. This explains the difference in pericynthion altitude deviation for translunar MCC-4 (table X) and LOI(1) (table XII). The error given for perigee altitude in table XII after LOI(1) is chiefly the propagated effect of the initial state vector uncertainty caused primarily by venting. In fact, the most notable trajectory deviations following the LOI(1) maneuver are a result of these initial state vector uncertainties. However, dispersions in perigee altitude after the LOI(1) maneuver are small enough to insure a safe lunar orbit.

LOI(2)

Cross-axis velocity residuals are the most significant errors occurring from the LOI(2) maneuver dispersion analysis presented in table XIII. The 3σ cross-axis velocity error for this maneuver is about 3 fps and is due to initial thrust vector mistrim.

TEI

The dispersion data presented in table XIV is for the transearth injection maneuver (TEI). This maneuver appears to be most sensitive to in-plane velocity errors. The inertial velocity error is approximately the same as the in-plane incremental velocity error.

Tranearth Phase

Four transearth midcourse correction maneuvers are presented in tables XV through XVIII. The targets used were determined by targeting 3σ dispersed translunar trajectories to a nominal entry flight-path angle of -6.249° . The most significant dispersions for all of the transearth midcourse correction maneuvers are in the resulting entry flight-path angle.

After the first transearth midcourse maneuver (table XV), the 3σ deviation in entry flight-path angle is 2.48° , which is outside of the entry corridor (-5.7° to -7.3°). The 3σ deviation in entry flight-path angle for the second transearth midcourse maneuver (table XVI) is 2.08° , which is still outside the entry corridor. After the third transearth midcourse maneuver (table XVII), the 3σ deviation in entry flight-path angle is $\pm 0.67^\circ$, which is within the entry corridor. Also, after the

fourth transearth midcourse maneuver (table XVIII), the 3σ deviation in entry flight-path angle of $\pm 0.159^\circ$ is well within the entry corridor.

The inertial velocity at entry interface (400 000-ft altitude) ranges from 36 067 fps to 36 075 fps in the worst case. A detailed analysis of the transearth dispersions is presented in reference 2, and is summarized in table XX.

The dispersion analysis of the reentry phase presented in table XIX shows that the 3σ deviation down range from the nominal landing point is ± 6.3 n. mi. The 3σ cross-range deviation is ± 5.6 n. mi. More detailed reentry dispersions are presented in reference 5.

CONCLUSIONS

As a result of this dispersion analysis it can be concluded that

1. Velocity residuals will occur for SPS short burns in the range of from 1 to 6 seconds because the CMC does not adequately model the total impulse of the SPS engine used. These residuals are a function of burn time.
2. The effects of continuous spacecraft venting along the velocity vector on the MSFN navigation uncertainties during translunar flight cause large deviations in pericynthion altitude.
3. Dispersions in perigee altitude following LOI(1) are small enough to insure a safe lunar orbit.
4. The 3σ flight-path angle and inertial velocity at entry interface are well within the entry corridor.
5. The 3σ range of landing point dispersions is ± 6.3 n. mi. down range and ± 5.6 n. mi. cross range.

TABLE I.- COVARIANCE MATRIX OF ACTUAL STATE VECTOR DEVIATIONS

AT TLI CUTOFF-PLUS-15-MINUTES^a[U-V-W system; 1σ](a) Covariance matrix^b

$$\left[\begin{array}{ccc} .18040878+10 & & \\ .25065182+10 & .72569522+10 & \\ -.57959265+08 & -.19792001+08 & .71454896+09 \\ -.13366415+07 & -.44414327+07 & -.71690395+05 \\ -.25669476+05 & .18033320+07 & -.38816033+04 \\ .88471992+04 & .14136089+06 & .52234188+06 \end{array} \right] \quad \left[\begin{array}{ccc} .27755400+04 & & \\ -.12376235+04 & .90161905+03 & \\ -.14813888+03 & .34784812+02 & .39252955+03 \end{array} \right]$$

(b) State vector deviations

$U = 42 \text{ ft}$

$\dot{U} = 52.68 \text{ fps}$

$V = 85 \text{ ft}$

$\dot{V} = 30.02 \text{ fps}$

$W = 26 \text{ ft}$

$\dot{W} = 19.81 \text{ fps}$

^aIncludes all deviations due to dispersions in the launch vehicle system from liftoff.^bSymmetric.

TABLE II.- COVARIANCE MATRIX OF ACTUAL STATE VECTOR UNCERTAINTIES

AT NOMINAL LOI(1) IGNITION^a[U-V-W system; 1σ](a) Covariance matrix^b

$$\begin{bmatrix} .85845272+08 & & \\ -.10145939+09 & .12674485+09 & \\ -.26674137+08 & .62081905+08 & .14509805+09 \\ .85935943+05 & -.10562061+06 & -.44853834+05 \\ -.36733660+05 & .42845849+05 & .88855644+04 \\ .27691676+05 & -.62993942+05 & -.14411066+06 \end{bmatrix}$$

(b) State vector deviations

$U = 9 \text{ } 265.27 \text{ ft} \quad \dot{U} = 9.40 \text{ fps}$

$V = 1 \text{ } 125.81 \text{ ft} \quad \dot{V} = 3.97 \text{ fps}$

$W = 12 \text{ } 045.66 \text{ ft} \quad \dot{W} = 11.96 \text{ fps}$

^aState vector uncertainties include the effects of venting during translunar coast. Venting was modeled as a continuous thrust of 0.0125 lb along the down-range velocity component (worst case consideration).

^bSymmetric.

TABLE III.- COVARIANCE MATRIX OF ACTUAL STATE VECTOR
DEVIATIONS AT NOMINAL LOI(2) IGNITION

[U-V-W system; 1σ]

(a) Covariance matrix^a

$$\begin{bmatrix} \cdot 31221499+07 & \cdot 34350225+08 & \\ \cdot 21214753+07 & \cdot 41978861+08 & \\ \cdot 59282900+05 & \cdot 91719200+06 & \\ \cdot 40228000+04 & \cdot 30303700+05 & \cdot 57129999+03 \\ \cdot 26109999+04 & \cdot 27428000+04 & \cdot 70969999+02 \\ \cdot 1950000+03 & \cdot 12582999+04 & \cdot 44366699+05 \end{bmatrix} \begin{bmatrix} \cdot 29958000+02 & \cdot 2561700-01 & \\ \cdot 40000000+01 & \cdot 50000000+00 & \\ \cdot 00000000 & \cdot 48827999+02 \end{bmatrix}$$

(b) State vector deviations

$$U = 1766.96 \text{ ft} \quad \dot{U} = 5.47 \text{ fps}$$

$$V = 5860.90 \text{ ft} \quad \dot{V} = 0.16 \text{ fps}$$

$$W = 6479.10 \text{ ft} \quad \dot{W} = 6.98 \text{ fps}$$

^aSymmetric.

TABLE IV.- COVARIANCE MATRIX OF ACTUAL STATE VECTOR

DEVIATIONS AT NOMINAL TEI IGNITION

[X-Y-Z system; 1σ]

(a) Covariance matrix^a

$$\begin{bmatrix} .30456828+07 & .26246079+08 & .28454785+08 \\ -.39140081+07 & .14925800+06 & .16376500+05 \\ .44250897+06 & .17352400+05 & .12980000+01 \\ -.69200000+03 & .13976960+05 & .189938+02 \\ -.56735550+03 & -.16596577+05 & .24951000+05 \\ .42699999+04 & -.16596577+05 & .69759999+01 \end{bmatrix}$$

(b) State vector deviations

$$U = 1745.18 \text{ ft} \quad \dot{U} = 4.86 \text{ fps}$$

$$V = 5123.09 \text{ ft} \quad \dot{V} = 4.35 \text{ fps}$$

$$W = 5334.30 \text{ ft} \quad \dot{W} = 6.65 \text{ fps}$$

^aSymmetric.

TABLE V.- COVARIANCE MATRIX OF ACTUAL STATE VECTOR
DEVIATIONS AT NOMINAL TEI CUTOFF-PLUS-10-SECONDS

[U-V-W system; 1σ]

(a) Covariance matrix^a

$$\left[\begin{array}{ccc} .32040386+07 & .24559743+08 & .51093979+08 \\ -.50283479+06 & .17624099+07 & -.19161275+04 \\ -.15565214+07 & -.22041844+05 & -.13926632+04 \\ .29188489+04 & .19799031+04 & .51494457+05 \\ -.29428234+04 & .46258218+04 & .4013200+01 \\ -.21132972+04 & & .7136729+02 \end{array} \right]$$

(b) State vector deviations

$$U = 1789.98 \text{ ft} \quad \dot{U} = 5.32 \text{ fps}$$

$$V = 4985.77 \text{ ft} \quad \dot{V} = 2.52 \text{ fps}$$

$$W = 7148.00 \text{ ft} \quad \dot{W} = 8.44 \text{ fps}$$

^aSymmetric.

TABLE VI.- TRANSLUNAR INJECTION DISPERSIONS

| Parameter (geocentric) | Nominal | $\pm 3\sigma$ deviation |
|-----------------------------------|---------------|--------------------------|
| Inertial velocity, fps | 35 555.90 | +43.50 -38.01 |
| Radius, ft | 21 998 516.00 | +43 074.00 -49 933.00 |
| Flight-path angle, deg | 7.21 | +0.483 -0.549 |
| Inclination, deg | 34.19 | +0.129 -0.120 |
| Longitude of descending node, deg | 123.85 | +0.150 -0.120 |
| Perigee altitude, n. mi. | 118.10 | +1.89 -3.36 |
| Apogee altitude, n. mi. | 291 770.00 | +10 529.00 -13 751.00 |
| Argument of perigee, deg | 153.35 | +0.30 -0.39 |
| Time at TLI, sec g.e.t. | 15 854.69 | +10.32 -13.38 |

TABLE VII.- TRANSLUNAR MCC-1 DISPERSIONS

[SPS maneuver]

| Parameter (geocentric) | Mean | 3σ deviation |
|--|----------------------|---------------------|
| Inertial velocity, fps | 9206.25 | 1.71 |
| Altitude, ft | 2.5959×10^8 | 84.90 |
| Flight-path angle, deg | 72.080 | 0.009 |
| Inclination, deg | 30.398 | 0.039 |
| Right ascension of ascending node, n. mi. | 141.59 | 0.00 |
| Pericynthion altitude, n. mi. | 60.30 | 72.21 |
| SPS propellant used for burn, lb | 539.26 | 8.73 |
| Cumulative SPS propellant used for burns, lb | 539.26 | 8.73 |
| Cumulative RCS propellant used for burns, lb | 0.000 | 0.00 |
| Burn time, sec | 8.11 | 0.15 |
| Sensed ΔV_x^a , fps | 67.21 | 1.08 |
| Sensed ΔV_y^a , fps | -4.37 | 0.24 |
| Sensed ΔV_z^a , fps | 55.76 | 0.84 |
| Sensed ΔV magnitude, fps | 87.44 | 1.32 |
| $V_{g(x)}$ residual ^b , fps | 0.08 | 1.32 |
| $V_{g(y)}$ residual ^b , fps | -0.04 | 1.87 |
| $V_{g(z)}$ residual ^b , fps | -0.05 | 1.71 |
| Inner gimbal angle, deg | -154.67 | 0.51 |
| Middle gimbal angle, deg | -6.74 | 0.54 |
| Outer gimbal angle, deg | -2.07 | -0.57 |

^aAccumulated ΔV in local vertical, local horizontal coordinates.^b V_g residuals in spacecraft control axis coordinates.

TABLE VIII.- TRANSLUNAR MCC-2 DISPERSIONS

[RCS maneuver]

| Parameter (geocentric) | Mean | 3σ deviation |
|--|-----------------------|---------------------|
| Inertial velocity, fps | 4925.19 | 0.78 |
| Altitude, ft | 6.85494×10^8 | 50.25 |
| Flight-path angle, deg | 77.297 | 0.009 |
| Inclination, deg | 31.445 | 0.045 |
| Right ascension of ascending node, deg | 142.20 | 0.03 |
| Pericynthion altitude, n. mi. | 60.30 | 38.64 |
| RCS propellant used for burn, lb | 27.41 | 6.03 |
| Cumulative SPS propellant used for burns, lb | 539.26 | 8.73 |
| Cumulative RCS propellant used for burns, lb | 27.41 | 6.03 |
| Burn time, sec | 37.94 | 8.43 |
| Sensed ΔV_x^a , fps | 3.04 | 0.90 |
| Sensed ΔV_y^a , fps | 0.20 | 0.75 |
| Sensed ΔV_z^a , fps | 2.44 | 0.81 |
| Sensed ΔV magnitude, fps | 3.92 | 0.87 |
| $V_g(x)$ residual ^b , fps | 0.00 | 0.00 |
| $V_g(y)$ residual ^b , fps | 0.00 | 0.00 |
| $V_g(z)$ residual ^b , fps | 0.00 | 0.00 |
| Inner gimbal angle, deg | 148.19 | 19.05 |
| Middle gimbal angle, deg | 48.82 | 13.59 |
| Outer gimbal angle, deg | 79.87 | 14.55 |

^a Accumulated ΔV in local vertical, local horizontal coordinates.

^b V_g residuals in spacecraft control axis coordinates.

TABLE IX.- TRANSLUNAR MCC-3 DISPERSIONS
[SPS maneuver]

| Parameter (geocentric) | Mean | 3σ deviation |
|--|--------------------|---------------------|
| Inertial velocity, fps | 3 616.70 | 1.02 |
| Altitude, ft | 159 373.32 | 0.00 |
| Flight-path angle, deg | Not calculated | Not calculated |
| Inclination, deg | Not calculated | Not calculated |
| Right ascension of ascending node, deg | Not calculated | Not calculated |
| Pericynthion altitude, n. mi. | 60.30 | 33.90 |
| SPS propellant used for burn, lb | 52.15 | 8.01 |
| Cumulative SPS propellant used for burns, lb | 591.41 | 17.04 |
| Cumulative RCS propellant used for burns, lb | 27.41 | 6.03 |
| Burn time, sec | 0.64 | 0.00 |
| Sensed ΔV_x^a , fps | 7.47 | 1.02 |
| Sensed ΔV_y^a , fps | 0.00 | 0.00 |
| Sensed ΔV_z^a , fps | 0.00 | 0.00 |
| Sensed ΔV magnitude, fps | 7.47 | 1.02 |
| $v_g(x)$ residual ^b , fps | ^c -2.13 | ^c 1.04 |
| $v_g(y)$ residual ^b , fps | 0.00 | 0.00 |
| $v_g(z)$ residual ^b , fps | 0.00 | 0.00 |
| Inner gimbal angle, deg | Not calculated | Not calculated |
| Middle gimbal angle, deg | Not calculated | Not calculated |
| Outer gimbal angle, deg | Not calculated | Not calculated |

^aAccumulated ΔV in local vertical, local horizontal coordinates.

^b v_g residuals in spacecraft control axis coordinates.

^cComputed from minimum impulse curves given in reference 3; also includes 0.14-second delay in engine cutoff (PRELIMINARY DATA).

TABLE X.- TRANSLUNAR MCC-4 DISPERSIONS
[SPS maneuver]

| Parameter (selenocentric) | Mean | 3σ deviation |
|--|--------------------|---------------------|
| Inertial velocity, fps | 3 964.18 | 1.35 |
| Altitude, ft | 20 351.91 | 0.00 |
| Flight-path angle, deg | Not calculated | Not calculated |
| Inclination, deg | Not calculated | Not calculated |
| Right ascension of ascending node, deg | Not calculated | Not calculated |
| Pericynthion altitude, n. mi. | 60.30 | 20.10 |
| SPS propellant used for burn, lb | 202.91 | 4.50 |
| Cumulative SPS propellant used for burns, lb | 794.32 | 21.54 |
| Cumulative RCS propellant used for burns, lb | 27.41 | 6.03 |
| Burn time, sec | 3.34 | 0.00 |
| Sensed ΔV_x^a , fps | 6.14 | 1.20 |
| Sensed ΔV_y^a , fps | -21.39 | 1.35 |
| Sensed ΔV_z^a , fps | -24.40 | 1.35 |
| Sensed ΔV magnitude, fps | 32.88 | 1.35 |
| $V_g(x)$ residual ^b , fps | ^c -5.47 | 1.35 |
| $V_g(y)$ residual ^b , fps | 0.02 | 0.00 |
| $V_g(z)$ residual ^b , fps | 0.12 | 0.00 |
| Inner gimbal angle, deg | Not calculated | Not calculated |
| Middle gimbal angle, deg | Not calculated | Not calculated |
| Outer gimbal angle, deg | Not calculated | Not calculated |

^aAccumulated ΔV in local vertical, local horizontal coordinates.

^b V_g residuals in spacecraft control axis coordinates.

^cIncludes tailoff impulse = 10 500 lb-second and also a 0.14-second delay in SPS engine cutoff (PRELIMINARY DATA).

TABLE XI.- SUMMARY OF TRANSLUNAR PHASE DISPERSION RESULTS^a

| Dispersions | Maneuver | | | |
|---|----------|-------|-------|-------|
| | MCC-1 | MCC-2 | MCC-3 | MCC-4 |
| Percent SPS maneuvers performed | 95 | 0 | 1.5 | 55.5 |
| SPS ΔV (3σ), fps | 87.45 | 0 | 5.34 | 28.71 |
| SPS burn time (3σ), sec | 8.11 | 0 | 0.64 | 3.34 |
| Percent RCS maneuvers performed | 4 | 46 | 80 | 44.5 |
| Percent RCS trims performed | 72 | 0 | 1.5 | 55.5 |
| Percent no maneuvers performed | 1 | 54 | 18.5 | 0 |
| RCS ΔV (3σ), fps | 4.65 | 3.89 | 4.64 | 4.78 |
| RCS burn time (3σ), sec | 50.97 | 37.94 | 45.66 | 53.40 |
| Pericynthion altitude (3σ), n. mi. | 72.10 | 38.64 | 33.90 | 20.10 |

^aSummary of results of end-to-end dispersion analysis given in reference 2.

TABLE XII.- LOI(1) DISPERSIONS

[SPS maneuver]

| Parameter (selenocentric) | Mean | 3σ deviation |
|--|--------------|---------------------|
| Inertial velocity, fps | 5 481.83 | 14.37 |
| Altitude, ft | 358 424.09 | 24 572.67 |
| Flight-path angle, deg | -0.36 | 0.096 |
| Inclination, deg | 146.31 | 0.180 |
| Right ascension of ascending node, deg | 187.85 | 0.87 |
| Perigee altitude, n. mi. | 58.59 | 3.93 |
| Apogee altitude, n. mi. | 168.65 | 5.43 |
| Semimajor axis, ft | 6 392 759.70 | 24 833.01 |
| SPS propellant used for burn, lb | 16 042.06 | 80.97 |
| Cumulative SPS propellant used for burns, lb | 16 836.38 | 102.51 |
| Cumulative RCS propellant used for burns, lb | 27.41 | 6.03 |
| Spacecraft weight, lb | 46 584.71 | 142.02 |
| Burn time, sec | 241.11 | 2.46 |
| Sensed ΔV_x^a , fps | -2 953.33 | 5.10 |
| Sensed ΔV_y^a , fps | 232.73 | 7.71 |
| Sensed ΔV_z^a , fps | -411.43 | 6.48 |
| Sensed ΔV magnitude, fps | 2 990.88 | 5.10 |
| $V_g(x)$ residual ^b , fps | -0.04 | 1.65 |
| $V_g(y)$ residual ^b , fps | 0.00 | 0.00 |
| $V_g(z)$ residual ^b , fps | 0.00 | 0.00 |
| Inner gimbal angle, deg | -165.01 | 0.09 |
| Middle gimbal angle, deg | 6.92 | 0.09 |
| Outer gimbal angle, deg | -179.50 | 0.51 |

^aAccumulated ΔV in local vertical, local horizontal coordinates.^b V_g residuals in spacecraft control axis coordinates.

TABLE XIII.- LOI(2) DISPERSIONS

[SPS maneuver]

| Parameter (selenocentric) | Mean | 3σ deviation |
|--|--------------|---------------------|
| Inertial velocity, fps | 5 344.09 | 5.65 |
| Altitude, ft | 358 691.24 | 5 924.82 |
| Flight-path angle, deg | 0.006 | 0.069 |
| Inclination, deg | 146.307 | 0.270 |
| Right ascension of ascending node, deg | 187.91 | 0.09 |
| Perigee altitude, n. mi. | 58.26 | 1.62 |
| Apogee altitude, n. mi. | 59.35 | 1.05 |
| Semimajor axis, ft | 6 059 703.30 | 5 740.29 |
| SPS propellant used for burn, lb | 633.66 | 9.12 |
| Cumulative SPS propellant used for burns, lb | 17 470.04 | 111.63 |
| Cumulative RCS propellant used for burns, lb | 27.41 | 6.03 |
| Spacecraft weight, lb | 45 930.79 | 167.07 |
| Burn time, sec | 9.53 | 0.15 |
| Sensed ΔV_x^a , fps | -138.51 | 1.80 |
| Sensed ΔV_y^a , fps | 0.00 | 0.33 |
| Sensed ΔV_z^a , fps | -1.22 | 0.30 |
| Sensed ΔV magnitude, fps | 138.52 | 1.80 |
| $V_g(x)$ residual ^b , fps | -0.01 | 1.80 |
| $V_g(y)$ residual ^b , fps | -0.01 | 2.28 |
| $V_g(z)$ residual ^b , fps | 0.05 | 2.25 |
| Inner gimbal angle, deg | -0.01 | 0.39 |
| Middle gimbal angle, deg | 0.00 | 0.39 |
| Outer gimbal angle, deg | 0.00 | 0.03 |

^aAccumulated ΔV in local vertical, local horizontal coordinates.^b V_g residuals in spacecraft control axis coordinates.

TABLE XIV.- TEI DISPERSIONS
[SPS maneuver]

| Parameter (selenocentric) | Mean | 3σ deviation |
|--|------------|---------------------|
| Inertial velocity, fps | 8 168.31 | 7.32 |
| Altitude, ft | 376 616.25 | 5382.72 |
| Flight-path angle, deg | 3.492 | 0.078 |
| Inclination, deg | 146.596 | 0.195 |
| Right ascension of ascending node, deg | 188.22 | 0.33 |
| SPS propellant used for burn, lb | 11 178.92 | 63.45 |
| Cumulative SPS propellant used for burns, lb | 28 648.96 | 175.08 |
| Cumulative RCS propellant used for burns, lb | 27.41 | 6.03 |
| Spacecraft weight, lb | 34 484.21 | 140.64 |
| Burn time, sec | 168.02 | 1.74 |
| Sensed ΔV_x^a , fps | 2 820.55 | 4.02 |
| Sensed ΔV_y^a , fps | 28.98 | 9.96 |
| Sensed ΔV_z^a , fps | 312.41 | 6.78 |
| Sensed ΔV magnitude, fps | 2 837.95 | 3.96 |
| $v_g(x)$ residual ^b , fps | -0.12 | 2.22 |
| $v_g(y)$ residual ^b , fps | 0.00 | 0.00 |
| $v_g(z)$ residual ^b , fps | 0.00 | 0.00 |
| Inner gimbal angle, deg | 42.05 | 0.06 |
| Middle gimbal angle, deg | 0.67 | 0.06 |
| Outer gimbal angle, deg | -0.08 | 0.36 |

^aAccumulated ΔV in local vertical, local horizontal coordinates.

^b v_g residuals in spacecraft control axis coordinates.

TABLE XV.- TRANSEARTH MCC-1 DISPERSIONS

[RCS maneuver]

| Parameter (selenocentric) | Mean | 3σ deviation |
|--|----------------------|---------------------|
| Inertial velocity, fps | 3 443.51 | 1.14 |
| Altitude, ft | 1.2165×10^8 | 16.20 |
| Flight-path angle, deg | 83.998 | 0.018 |
| Inclination, deg | 146.646 | 0.153 |
| Right ascension of ascending node, deg | 188.12 | 0.27 |
| Entry flight-path angle, deg | -6.249 | 2.481 |
| RCS propellant used for burn, lb | 39.75 | 4.44 |
| Cumulative SPS propellant used for burns, lb | 28 648.96 | 175.08 |
| Cumulative RCS propellant used for burns, lb | 67.16 | 10.47 |
| Burn time, sec | 55.01 | 6.12 |
| Sensed ΔV_x^a , fps | -4.15 | 1.11 |
| Sensed ΔV_y^a , fps | 0.88 | 1.32 |
| Sensed ΔV_z^a , fps | -9.31 | 1.44 |
| Sensed ΔV magnitude, fps | 10.24 | 1.44 |
| $V_g(x)$ residual ^b , fps | 0.00 | 0.00 |
| $V_g(y)$ residual ^b , fps | 0.00 | 0.00 |
| $V_g(z)$ residual ^b , fps | 0.00 | 0.00 |
| Inner gimbal angle, deg | 24.37 | 6.84 |
| Middle gimbal angle, deg | 5.51 | 7.74 |
| Outer gimbal angle, deg | -168.83 | 0.72 |

^aAccumulated ΔV in local vertical, local horizontal coordinates.^b V_g residuals in spacecraft control axis coordinates.

TABLE XVI.- TRANSEARTH MCC-2 DISPERSIONS
[RCS maneuver]

| Parameter (geocentric) | Mean | 3σ deviation |
|--|------------------------|---------------------|
| Inertial velocity, fps | 2 750.77 | 0.36 |
| Altitude, ft | 1.010913×10^9 | 15.27 |
| Flight-path angle, deg | -75.319 | 0.009 |
| Inclination, deg | 26.628 | 0.033 |
| Right ascension of ascending node, deg | 2.22 | 0.03 |
| Entry flight-path angle, deg | -6.249 | 2.079 |
| RCS propellant used for burn, lb | 13.47 | 1.44 |
| Cumulative SPS propellant used for burns, lb | 28 648.96 | 175.08 |
| Cumulative RCS propellant used for burns, lb | 80.63 | 11.91 |
| Burn time, sec | 18.65 | 2.04 |
| Sensed ΔV_x^a , fps | 3.47 | 0.36 |
| Sensed ΔV_y^a , fps | -0.01 | 0.42 |
| Sensed ΔV_z^a , fps | -0.00 | 0.36 |
| Sensed ΔV magnitude, fps | 3.47 | 0.36 |
| $V_g(x)$ residual ^b , fps | 0.00 | 0.00 |
| $V_g(y)$ residual ^b , fps | 0.00 | 0.03 |
| $V_g(z)$ residual ^b , fps | 0.00 | 0.03 |
| Inner gimbal angle, deg | -150.75 | 7.29 |
| Middle gimbal angle, deg | -5.91 | 8.07 |
| Outer gimbal angle, deg | 175.37 | 0.75 |

^aAccumulated ΔV in local vertical, local horizontal coordinates.

^b V_g residuals in spacecraft control axis coordinates.

TABLE XVII.- TRANSEARTH MCC-3 DISPERSIONS

[RCS maneuver]

| Parameter (geocentric) | Mean | 3σ deviation |
|--|----------------------|---------------------|
| Inertial velocity, fps | 4 249.01 | 0.30 |
| Altitude, ft | 7.2575×10^8 | 14.44 |
| Flight-path angle, deg | -76.182 | 0.003 |
| Inclination, deg | 26.619 | 0.021 |
| Right ascension of ascending node, deg | 2.25 | 0.00 |
| Entry flight-path angle, deg | -6.249 | 0.669 |
| RCS propellant used for burn, lb | 10.91 | 1.17 |
| Cumulative SPS propellant used for burns, lb | 28 648.96 | 175.08 |
| Cumulative RCS propellant used for burns, lb | 91.54 | 13.05 |
| Burn time, sec | 15.10 | 1.65 |
| Sensed ΔV_x^a , fps | 2.81 | 0.30 |
| Sensed ΔV_y^a , fps | -0.01 | 0.36 |
| Sensed ΔV_z^a , fps | 0.01 | 0.30 |
| Sensed ΔV magnitude, fps | 2.81 | 0.30 |
| $V_g(x)$ residual ^b , fps | 0.00 | 0.00 |
| $V_g(y)$ residual ^b , fps | 0.00 | 0.00 |
| $V_g(z)$ residual ^b , fps | 0.00 | 0.00 |
| Inner gimbal angle, deg | -145.79 | 6.63 |
| Middle gimbal angle, deg | -6.25 | 7.77 |
| Outer gimbal angle, deg | 175.93 | 0.72 |

^aAccumulated ΔV in local vertical, local horizontal coordinates.^b V_g residuals in spacecraft control axis coordinates.

TABLE XVIII.- TRANSEARTH MCC-4 DISPERSIONS

[RCS maneuver]

| Parameter (geocentric) | Mean | 3σ deviation |
|--|----------------------|---------------------|
| Inertial velocity, fps | 14 025.33 | 0.78 |
| Altitude, ft | 1.0909×10^8 | 35.61 |
| Flight-path angle, deg | -65.205 | 0.003 |
| Inclination, deg | 26.611 | 0.006 |
| Right ascension of ascending node, deg | 2.28 | 0.000 |
| Entry velocity, fps | 36 070.98 | 3.93 |
| Entry flight-path angle, deg | -6.249 | 0.159 |
| RCS propellant used for burn, lb | 25.19 | 2.85 |
| Cumulative SPS propellant used for burns, lb | 28 648.96 | 175.08 |
| Cumulative RCS propellant used for burns, lb | 116.73 | 15.90 |
| Burn time, sec | 34.86 | 4.02 |
| Sensed ΔV_x^a , fps | 6.48 | 0.72 |
| Sensed ΔV_y^a , fps | -0.00 | 0.69 |
| Sensed ΔV_z^a , fps | -0.00 | 0.84 |
| Sensed ΔV magnitude, fps | 6.48 | 0.72 |
| $V_g(x)$ residual ^b , fps | 0.00 | 0.00 |
| $V_g(y)$ residual ^b , fps | 0.00 | 0.00 |
| $V_g(z)$ residual ^b , fps | 0.00 | 0.00 |
| Inner gimbal angle, deg | 126.60 | 7.11 |
| Middle gimbal angle, deg | 15.72 | 8.10 |
| Outer gimbal angle, deg | 103.93 | 1.95 |

^aAccumulated ΔV in local vertical, local horizontal coordinates.^b V_g residuals in spacecraft control axis coordinates.

TABLE XIX.- REENTRY DISPERSIONS^a

| Deviations in nominal landing point | |
|-------------------------------------|------|
| Down-range deviation, n. mi. | 6.30 |
| Cross-range deviation, n. mi. | 5.61 |

TABLE XX.- SUMMARY OF TRANSEARTH PHASE DISPERSIONS RESULTS^b

| Dispersions | Maneuver | | | |
|--|----------|-------|-------|-------|
| | MCC-1 | MCC-2 | MCC-3 | MCC-4 |
| Percent SPS maneuvers performed | .5 | 0 | 0 | 0 |
| SPS ΔV , fps (+ ullage) | 12.01 | 0 | 0 | 0 |
| SPS burn time, sec | 0.40 | 0 | 0 | 0 |
| Percent RCS maneuvers performed | 55 | 15.5 | 46 | 62 |
| Percent RCS trims | .5 | 0 | 0 | 0 |
| Percent no maneuvers performed | 44.5 | 84.5 | 54 | 38 |
| RCS ΔV (3σ), fps | 10.53 | 4.11 | 3.95 | 8.09 |
| RCS burn time (3σ), sec | 55.01 | 22.12 | 21.26 | 43.47 |
| Entry flight-path angle (3σ), deg | 2.48 | 2.08 | 0.67 | 0.16 |

^aReference 5.^bSummary of results of end-to-end dispersion analysis given in reference 2.

REFERENCES

1. LMAB: Apollo Mission C' Spacecraft Operational Trajectory, Alternate 1, Lunar Orbital Mission, Volume I - Mission Profile for a Mission Launched December 21, 1968. MSC IN 68-FM-252, October 25, 1968.
2. Hitt, G. C.; Kindall, S. M., TRW Systems Group; and Yencharis, J. D., LMAB: Apollo 8 Spacecraft Dispersion Analysis, Volume II - Translunar and Transearth Phases. MSC IN 68-FM-303, December 16, 1968.
3. MSC: CSM/LM Spacecraft Operational Data Book, Volume I - CSM Data Book. MSC document SNA-8-D-027(I), May 1968.
4. Graf, Otis F: Expected Errors in Apollo 8 Short SPS Burns. MSC memorandum 68-FM73-569, to be published.
5. Burton, J. K.: Landing Errors for the C Prime Mission. MSC memorandum 68-FM23-198, December 2, 1968.